

## The Nova Rate in M94 (NGC 4736)

T. Güth and A. W. Shafter

*Astronomy Department, San Diego State University, San Diego, CA 92182*

tgueth@sciences.sdsu.edu, aws@nova.sdsu.edu

and

K. A. Misselt

*Steward Observatory, University of Arizona, 933 North Cherry Avenue, Tucson, AZ 85721*

misselt@as.arizona.edu

### ABSTRACT

A multi-epoch H $\alpha$  survey of the early-type spiral galaxy M94 (NGC 4736) has been completed as part of a program to establish the galaxy's nova rate. A total of four nova candidates were discovered in seven epochs of observation during the period from 2005 to 2007. After making corrections for temporal coverage and spatial completeness, a global nova rate of  $5.0^{+1.8}_{-1.4}$  yr $^{-1}$  was determined. This rate corresponds to a specific-luminosity nova rate of  $1.4 \pm 0.5$  novae per year per  $10^{10} L_{\odot,K}$  when the  $K$  luminosity is determined from the  $B - K$  color, or  $1.5 \pm 0.4$  novae per year per  $10^{10} L_{\odot,K}$  when the  $K$  luminosity is derived from the Two Micron All Sky Survey. These values are slightly lower than that of other galaxies with measured nova rates, which typically lie in the range of 2 – 3 novae per year per  $10^{10} L_{\odot}$  in the  $K$  band.

*Subject headings:* galaxies: individual (M94) — novae, cataclysmic variables

### 1. Introduction

Novae, a subclass of cataclysmic variables, occur in semidetached binary systems where a white dwarf primary star accretes material from its Roche lobe-filling late-type companion (e.g., see Warner 1995). When the mass accretion rate is sufficiently low, the accreted material builds up on the surface of the white dwarf under degenerate conditions. A thermonuclear runaway (TNR) eventually ensues when the temperature and density at the base of the accreted material become sufficiently high. The TNR causes the accreted material to be blown off, resulting in an outburst of 10 – 20 mag. The corresponding peak luminosity can be as high as  $M_V \sim -10$ , and visible in galaxies as distant as the Virgo cluster. The properties of nova eruptions (peak luminosity and fade rate) are expected to be strongly dependent on properties such as the mass accretion rate,

the luminosity and the mass of the WD, which are expected to change with the underlying stellar populations (e.g. Shara et al. 1980; Prialnik et al. 1982; Livio 1992).

In a seminal paper, Yungelson et al. (1997) presented the results of stellar population synthesis models that predicted the infrared (e.g.,  $K$  band) luminosity-specific nova rate (LSNR) of a galaxy should have a strong dependence on the history of its star formation rate (SFR). This dependence is due to an expected increase in the average mass of the white dwarfs in nova binaries with decreasing time elapsed since the zero-age main-sequence system formed (Tutukov & Yungelson 1995). Since higher mass white dwarfs exhibit more frequent, and more luminous, nova eruptions (Ritter et al. 1991; Livio 1992; Kolb 1995), elliptical galaxies, which form most of their stars in an early burst of star formation, were not expected to be prolific nova producers. Alternatively, galaxies that have formed a significant fraction of their stars relatively recently, like late-type spiral galaxies, were predicted to have higher observed LSNRs. In addition to Hubble type, the LSNRs of galaxies were also expected to be dependent on galaxy mass. Over their lifetimes, dwarf, late-type spiral galaxies are believed to have an almost constant SFR, while their giant, late-type counterparts are thought to have star formation rates that are exponentially decaying (Gavazzi & Scodregigo 1996). Thus, massive spiral galaxies are predicted to have less active SFRs due to low LSNRs when compared with the dwarf spiral and irregular systems.

Over the past two decades, nova surveys have been conducted in galaxies spanning a wide range of Hubble types. In an early study based on a limited sample of galaxies, Ciardullo et al. (1990a) concluded that the  $K$ -band LSNR was basically independent of Hubble type. Shortly thereafter, Della Valle et al. (1994) re-analyzed many of these same galaxies and reached a somewhat different conclusion; namely, that the LSNRs are systematically higher in the late-type, low-mass spiral galaxies, such as M33, the Large Magellanic Cloud (LMC), and the Small Magellanic Cloud (SMC), consistent with the predictions of the synthesis models subsequently published by Yungelson et al. (1997). A principal limitation of these early studies was the lack of data for massive, late-type spiral galaxies for which nova rates had yet to be determined. With this in mind, Shafter et al. (2000) surveyed two massive, late-type spirals, M51 and M101, and, for comparison, the giant Virgo elliptical galaxy, M87, finding a slightly higher LSNR for M87 than for either of the massive spirals M51 or M101 (the difference, however, was not statistically significant). In more recent years several additional nova surveys have been conducted (Shara & Zurek 2002; Ferrarese et al. 2003; Williams & Shafter 2004; Coelho et al. 2008). Like Shafter et al. (2000), most of these studies failed to find any convincing variation of the LSNR with Hubble type. However, large uncertainties in the LSNRs for many galaxies remain, with, for example, published nova rates for the giant Virgo elliptical M87 varying by as much as a factor of 3 (Shafter et al. 2000; Shara & Zurek 2002).

To make further progress in understanding what effect, if any, the underlying stellar population might have on the LSNR it is important to obtain nova rates for additional galaxies spanning a broad range of Hubble types. With this motivation in mind, we have conducted a survey for novae in the early-type Sab galaxy M94 (NGC 4736), which is well known for its inner ring of ongoing starburst activity (Waller et al. 2001). Here we report the results of our survey.

## 2. Observations

Data for M94 were obtained over seven epochs spanning 2005 May to 2007 June using the Steward Observatory 2.3-m Bok Telescope. All observations were made with the 90Prime camera (Williams et al. 2004), consisting of an array of four  $4K \times 4K$  CCDs mounted at prime focus, giving a full field of view of  $\sim 1 \text{ deg}^2$ . For our observations, the  $\sim 30' \times 30'$  coverage provided by a single chip was sufficient to cover essentially the full disk of M94.

As emphasized by Ciardullo et al. (1990b) conducting nova surveys in  $H\alpha$  has several advantages over observations in the broadband continuum. Shortly after eruption, novae develop strong and broad ( $\gtrsim 1000 \text{ km s}^{-1}$ )  $H\alpha$  emission lines that fade slowly, normally requiring several months to decline by more than 2 mag. Thus, novae can be detected in  $H\alpha$  with less frequent temporal sampling. In addition, observations in  $H\alpha$  are also less affected by extinction than those in  $B$  light, which provides an added advantage for detection of novae in spiral galaxies. Finally, the narrow-band  $H\alpha$  observations facilitate the detection of novae against a bright background, particularly near the nuclei of galaxies. For these reasons, following our earlier work (e.g. Shafter et al. 2000; Coelho et al. 2008), observations of M94 were made using a narrow-band  $H\alpha$  filter having a central bandpass of  $6580 \text{ \AA}$  and a FWHM of  $\sim 80 \text{ \AA}$ .

Based on the distance modulus to M94, which we take to be  $\mu_0 = 28.21 \pm 0.07$  (Herrmann et al. 2008), we estimated that a total exposure time of  $\sim 2$  hr would allow us to reach a limiting absolute magnitude of  $M_{H\alpha} \sim -6.7$  ( $m_{H\alpha} \sim 21.5$ ) necessary to detect a significant fraction of the novae. Our target exposure time of 2 hr was divided into a series of individual 600–900 s exposures that were later median stacked in order to suppress cosmic ray artifacts and to avoid saturation of the brightest stars in the image. In addition, a set of sky flats, bias frames, and dark frames were obtained for each epoch of observation. The individual images were first de-biased and flat-fielded before a world coordinate system (WCS) was assigned to each image with the IRAF<sup>1</sup> routine `msctpeak` using coordinates from the US Naval Observatory A2 catalog. The images of a given epoch were then aligned using several stars common to each image. In four of the seven epochs, the galaxy was centered on a single chip (chip 1) in all exposures, allowing the images to be aligned with the IRAF routine `imalign`. In the remaining three epochs, exposures of M94 were alternated between three CCDs (chip 3 was excluded due to a large area of bad pixels). As a result, use of the IRAF routine `sregister`, which accounts for the slight rotation from one chip to another, was required to align these images. Individual images from a given observing run (whether a single night or two consecutive nights such as 2005 May 1 and 2, and 2005 May 30 and 31) were then combined into a single master image for that epoch. The resulting master images for each of seven epochs ended up representing between 1.67 and 3 hr of coverage. A summary of the observations can be found in Table 1.

---

<sup>1</sup>IRAF (Image Reduction and Analysis Facility) is distributed by the National Optical Astronomy Observatory, which is operated by Association of Universities for Research in Astronomy, Inc., under cooperative agreement with the National Science Foundation

## 2.1. Nova Detection

In order to search for novae most efficiently, the co-added images for all epochs separated by more than one year were spatially aligned and point-spread function (PSF) matched using the ISIS package (Alard & Lupton 1998). The resulting images were differenced in order to search for variable objects. To then qualify as a nova, an object had to appear in at least one epoch but not be present in other images obtained more than 6 months before or after the epoch of detection.

To confirm our nova candidates, and to search for any additional candidates that might have been missed, the images were also blinked by eye. Owing to the bright background galaxy light this procedure was ineffective within  $\sim 1.5'$  from the nucleus. For this inner region, we employed the IRAF `median` routine with a  $7 \times 7$  pixel box to generate smoothed background images that were then subtracted from their original images. These median subtracted images were then also blinked by eye. All four candidates were confirmed by the visual blinking process, but no further candidates were identified.

## 2.2. Nova Photometry

Photometry was performed using two different techniques. First, using the IRAF routine `psf` from the DAOPHOT package, raw magnitudes of the nova candidates were obtained. To confirm these measurements, the second IRAF routine used was `phot`, which is a simple aperture photometry method. We first had to extract  $100 \times 100$  sub-images centered on each nova and standard star due to the bright galactic background. Next, we excluded a 5 pixel radius aperture around the object and used the IRAF routine `imsurfit` to fit a two-dimensional surface to the background, which was then subtracted from the image. This left a flattened image on which aperture photometry was performed. Using apertures with diameter on the order of the seeing FWHM, we obtained the instrumental magnitudes for both the nova candidates and for a secondary standard star we defined, which is located at RA = 12hr 50m 48s.07, DECL =  $41^\circ 10' 06''.44$  (J2000). The secondary star was later calibrated ( $m_{H\alpha} = 15.71$ ) by comparison with the spectrophotometric standard star HZ 44 (Oke 1974) when both stars were observed under photometric conditions on the night of 2008 June 3 UT. This enabled us to convert the instrumental magnitudes of the novae to  $H\alpha$  magnitudes. In general, the magnitudes acquired from both the `psf` and `phot` methods were in agreement to within 0.1 mag. Hence, we used the mean value from the two readings unless they differed by more than 0.1 mag, in which case the `psf` value was adopted. In this study, we made the assumption that the  $H\alpha$  filter has a filling fraction of 100% as it has been done by Shafter & Irby (2001), Williams & Shafter (2004), and most recently by Coelho et al. (2008). The  $H\alpha$  emission line width changes from nova to nova, hence the bandpass can be underfilled, introducing a small error in the calibration. Nevertheless, making this assumption allows direct comparison with previous studies.

Table 2 lists the dates, positions, and  $H\alpha$  magnitudes of the four nova candidates discovered in this survey. M94N 2006-04a and M94N 2006-04b were detected in multiple epochs, but we

were unable to constrain the times of maximum light of these novae. Problems with the detector rendered our measurements from 2006 May uncertain. Nevertheless, our observations indicated that both of these nova candidates faded quite slowly. M94N 2006-04a faded by only about 0.5 mag in 60 days, raising the possibility that this transient source may not be a nova, but rather a luminous, long-period variable star. M94N 2006-04b is similar, but is more likely to be a slow nova considering that it declined faster and was almost a magnitude brighter at discovery, corresponding to an absolute magnitude of  $M_{H\alpha} \simeq -8.2$  at the distance of M94.

### 3. The Nova Rate in M94

To estimate the nova rate in M94, the completeness of the survey as a function of magnitude must be determined. We determined the completeness of our survey by performing artificial star tests using the IRAF routine `addstar` as in Williams & Shafter (2004) and Coelho et al. (2008). For 12 equally spaced magnitude bins, artificial novae with magnitudes ranging between  $m_{H\alpha} = 18.0$  and  $m_{H\alpha} = 23.0$  were created. Following the spatial distribution of the  $I$ -band light (from the data of Möllenhoff et al. (1995)), 100 artificial novae were randomly distributed throughout the image. The search for these artificial “novae” followed the same methods as the ones employed to determine the actual novae. This procedure, which was repeated three times and averaged, allowed us to construct a completeness function,  $C(m)$ , of the number of novae recovered in each magnitude bin, shown in Figure 1. The recovered novae fraction starts to decline steeply at magnitude of  $m_{H\alpha} \simeq 21.0$ . Following Shafter et al. (2000), Williams & Shafter (2004), and Coelho et al. (2008), we obtained the nova rate in M94 by employing two different procedures: a Monte Carlo simulation and a mean nova lifetime method.

#### 3.1. The Monte Carlo Procedure

We estimated the nova rate in M94 by employing a Monte Carlo simulation where the actual number of novae observed in this survey ( $n_{obs} = 4$ ) was compared with an estimate of the number of novae we could expect to see given an intrinsic nova rate,  $R$ . For a wide range of possible values of  $R$ , we computed a set of model  $H\alpha$  light curves based on randomly selected peak magnitudes and decay rates from a sample of detected novae in earlier studies of M31 (Shafter & Irby 2001) and M81 (Neill & Shara 2004). Based on the dates of our survey (Table 1) and our adopted distance to M94, we then computed an observed nova luminosity function,  $n(m, R)$ , for this range of possible nova rates. The resulting luminosity function was then convolved with the completeness function,  $C(m)$ , to determine the expected number of novae in M94:

$$N_{obs}(R) = \int C(m)n(m, R)dm \quad (1)$$

We repeated the Monte Carlo simulation  $10^6$  times and recorded the number of matches between  $N_{obs}(R)$  and  $n_{obs} = 4$ , the actual number of novae identified in this survey. We then normalized the number of matches as a function of  $R$ , and obtained the probability distribution function shown in Figure 2. The most probable nova rate, represented by the peak in the figure, is  $4.7_{-1.2}^{+1.6}$   $\text{yr}^{-1}$ , where the error range encompasses 50% of the integrated probability distribution. As we pointed out earlier, M94N 2006-04a has features that makes it difficult to confirm it as a nova candidate with complete confidence. If we exclude M94N 2006-04a, the nova rate drops as expected to  $3.4_{-0.9}^{+1.6}$   $\text{yr}^{-1}$ .

### 3.2. The Mean Nova Lifetime Procedure

We also determined an estimate of the nova rate using the mean nova lifetime method (Ciardullo et al. 1990b), which follows the original analysis by Zwicky (1942) to determine extragalactic supernova rates. Although this method is less sophisticated than the Monte Carlo procedure, it can be used as a check on our earlier results. We begin by expressing the nova rate,  $R$ , in the studied region as

$$R = \frac{N(M < M_c)}{T(M < M_c)} \quad (2)$$

where  $N(M < M_c)$  is the number of novae observed brighter than the limiting absolute magnitude  $M_c$  of the survey, and  $T(M < M_c)$  is the “effective survey time.” For multi-epoch surveys such as this survey, the effective survey time both depends on the mean nova lifetime,  $\tau_c$ , which is defined as the length of time a common nova remains brighter than  $M_c$ , and the frequency of sampling. Therefore:

$$T(M < M_c) = \tau_c + \sum_{i=2}^n \min(t_i - t_{i-1}, \tau_c) \quad (3)$$

where  $t_i$  is the time of the  $i$ th observation. Using observations from the bulge of M31, Shafter et al. (2000) provide a simple calibrated relationship between  $\tau_c$  and  $M_c$ , which we implement here:

$$\log \tau_c(\text{days}) \simeq (6.1 \pm 0.4) + (0.56 \pm 0.05)M_c \quad (4)$$

Adopting a limiting magnitude of  $m_{H\alpha} = 21.0$ ,  $\mu_0 = 28.21 \pm 0.07$ , and assuming a foreground extinction of  $\sim 0.08$  mag (Schegel et al. 1998), we estimate that  $M_c = -7.29 \pm 0.21$ . The mean nova lifetime and the effective survey time were calculated using the survey times provided in Table 1, and Equations (3) and (4), which yields  $\tau_c = 100.4 \pm 4.7$  days and  $T(M < M_c) = 480 \pm 14$  days,

respectively. Equation (2) provides a nova rate of  $3.0 \pm 1.5 \text{ yr}^{-1}$ . Given that we are only  $\sim 55\%$  complete down to our limiting magnitude of  $m_{\text{H}\alpha} = 21.0$  (see Figure 1), we estimate the nova rate in the surveyed region to be  $5.4 \pm 2.7$  nova per year. This nova rate agrees, within the margins of error, with the Monte Carlo nova rate value.

As with the Monte Carlo method, the mean nova lifetime rate was also determined excluding the uncertain nova M94N 2006-04a. Both the effective survey time and the mean nova lifetime are unaffected by the change in the number of nova candidates. In this case the nova rate drops to  $2.3 \pm 1.3 \text{ yr}^{-1}$ , or  $4.1 \pm 2.4 \text{ yr}^{-1}$  after correcting for the completeness at  $m_{\text{H}\alpha} = 21.0$ .

### 3.3. The Global Nova Rate

The large field of view of the 90Prime camera allows us to cover M94 almost completely, which requires only a small extrapolation to estimate the nova rate of the entire galaxy. Using the *I*-band photometry data of Möllenhoff et al. (1995) for M94, we estimate that  $\sim 95\%$  of the total infrared luminosity of the galaxy is included in the effective survey area, with an estimated  $\sim 5\%$  lost due to the placement of the galaxy on the CCD during some epochs of observation. Both the Monte Carlo and mean nova lifetime rates calculated above represent the rates in the surveyed region of M94 only, which need to be corrected for any fraction of the galaxy that falls outside the survey’s coverage. Assuming the 95% coverage, we obtain  $5.0^{+1.8}_{-1.4} \text{ yr}^{-1}$  and  $5.7 \pm 2.9 \text{ yr}^{-1}$  for the Monte Carlo global nova rate and mean nova lifetime global nova rate, respectively. If M94N 2006-04a is omitted, the estimate of the global nova rate based on the Monte Carlo and the mean nova lifetime drop to  $3.8^{+1.9}_{-1.1} \text{ yr}^{-1}$  and  $4.3 \pm 2.5 \text{ yr}^{-1}$ , respectively. These estimates have not been corrected for any extinction internal to M94, which is highly dependent on spatial position. In Figure 3, we have plotted the spatial distribution of all four nova candidates discovered in this survey over the *I*-band isophotes of M94 (Möllenhoff et al. 1995). Each isophote represents a 10% change in the total light of M94. The three strong nova candidates are represented by filled circles with the slowly fading nova candidate M94N 2006-04a represented by an open circle. All four nova candidates lie outside the inner starburst ring in M94, which has a diameter of approximately  $70''$ . The dotted square, which represents the size of the surveyed region, is a  $29' \times 29'$  region centered on the nucleus of the galaxy.

### 3.4. Luminosity-specific Nova Rate

To compare nova rates across different stellar populations, nova rates are typically normalized by the integrated infrared *K*-band luminosity of the galaxy, yielding a *K*-band luminosity-specific nova rate (LSNR),  $\nu_K$ , which is usually parameterized as the number of novae per year per  $10^{10} L_{\odot, K}$ .

There are two different ways to estimate the integrated *K*-band luminosity. The value can be

obtained directly from the Two Micron All Sky Survey’s (2MASS) Large Galaxy Atlas (Jarrett et al. 2003) or it can be estimated indirectly using the  $B$  integrated magnitude and  $(B - K)$  color. Although the 2MASS data provides direct  $K$  magnitude measurements of galaxies with determined nova rates, there are systematic differences between these values and those from the  $(B - K)$  color (Ferrarese et al. 2003; Williams & Shafter 2004; Coelho et al. 2008). Those discrepancies arise because the sky background levels near large galaxies are quite hard to measure accurately as pointed out by Williams & Shafter (2004). As a result, we consider the LSNR obtained from the galaxy colors to be more dependable, as concluded by Williams & Shafter (2004) and Coelho et al. (2008).

We adopt an integrated  $B$  magnitude for M94 of  $8.99 \pm 0.13$  (de Vaucouleurs et al. 1991). This value, coupled with a  $(B - K)$  color of  $3.72 \pm 0.10$  (Johnson 1966; de Vaucouleurs et al. 1991) yields an integrated  $K$ -band magnitude of  $5.18 \pm 0.016$ . At the distance of M94, our nova rate of  $5.0^{+1.8}_{-1.4}$  yr $^{-1}$  yields  $\nu_{K,\text{color}} = 1.4 \pm 0.5 \times 10^{-10} L_{\odot,K}^{-1}$  yr $^{-1}$ . If we were to adopt the revised  $K$  magnitude value of  $5.11 \pm 0.02$  from 2MASS, we find a slightly higher value of  $\nu_{K,2\text{MASS}} = 1.5 \pm 0.5 \times 10^{-10} L_{\odot,K}^{-1}$  yr $^{-1}$ . Finally, if we exclude M94N 2006-04a, we obtain  $\nu_{K,\text{color}} = 1.0 \pm 0.4 \times 10^{-10} L_{\odot,K}^{-1}$  yr $^{-1}$  and  $\nu_{K,2\text{MASS}} = 1.1 \pm 0.4 \times 10^{-10} L_{\odot,K}^{-1}$  yr $^{-1}$  for the galaxy colors and 2MASS estimates, respectively.

#### 4. Discussion

In an attempt to broaden the study of galaxies with different Hubble types, we have undertaken the first systematic survey for novae in the spiral galaxy M94. Figure 4 shows the LSNRs for M94 and other galaxies with measured nova rates plotted versus the  $B - K$  color of the host galaxy. Considering that only three of the four nova candidates in M94 may in fact be bona fide novae, we have plotted LSNRs appropriate for both possibilities. The data for all galaxies, except M94, are obtained from Tables 5 and 6 of Williams & Shafter (2004), and include the most recent LSNR value of M101 from Coelho et al. (2008).

Our best estimate of the LSNR for M94 ( $[1.4 \pm 0.5] \times 10^{-10} L_{\odot,K}^{-1}$  yr $^{-1}$ ) is in general agreement with the previous findings of Ciardullo et al. (1990a) and more recently with those of Shafter et al. (2000), Williams & Shafter (2004), and Coelho et al. (2008), who showed that the LSNR is remarkably insensitive to the Hubble type of the parent galaxy. Notable exceptions are apparently the Magellanic Clouds. The slightly higher rates for the LMC and the SMC can be broadly understood within the context of the population synthesis models of Yungelson et al. (1997) who argued that among late-type galaxies, the low-mass systems with their relatively constant star formation histories, should have generally higher LSNRs.

M94 is noted for a ring of active star formation with a diameter of  $\sim 70''$  surrounding the galaxy’s bright nucleus. Given the models of Yungelson et al. (1997), which predict a higher LSNR in galaxies with a recent history of star formation, it is perhaps surprising that the LSNR for M94 is not higher than those of galaxies with similar Hubble types, but with less active star formation.



In this regard, it is noteworthy that the four nova candidates discovered in our survey are located well outside the star-forming ring, and appear to have no association with it. Perhaps the relatively low LSNR for M94 and the lack of novae associated with the ring might be due to the difficulty in detecting nova candidates in the inner star-forming regions of the galaxy. Extinction internal to M94 may be significant, especially in the star-forming regions, and our inability to correct for it could lead to an underestimation of the nova rate. Further, we note that the adopted distance to M94 affects the derived LSNR. Although we use the most recent value by Herrmann et al. (2008), the distance to M94 is not well established. If we have underestimated the distance to M94, our derived nova rate will underestimate the galaxy’s true nova rate.

It is also possible that our limited temporal coverage might result in an underestimation of the actual nova rate of M94. Both the Monte Carlo and mean nova lifetime approaches attempt to correct for survey frequency, but both methods rely on an accurate knowledge of the nova light curve properties. A concern is whether the H $\alpha$  light curve data from M31 and M81 can be used in the Monte Carlo simulations for galaxies like M94 with differing Hubble types and SFRs. An H $\alpha$  survey of M81 with nearly continuous temporal coverage over a  $\sim 5$  month long period conducted by Neill & Shara (2004) showed that the LSNR of M81 is more than twice the value of that reported earlier by Moses & Shafter (1993). The authors argue that multi-epoch surveys have infrequent temporal coverage, which will systematically underestimate nova rates. However, Neill & Shara (2004) used a lower  $K$ -band luminosity for M81 that was adopted from the 2MASS data (Jarrett et al. 2003), which will increase their LSNR. If we adjust for this difference, the LSNR computed by Neill & Shara (2004) is only about  $\sim 40\%$  greater than the preliminary value found by Moses & Shafter (1993).

If the slightly low LSNR for M94 is confirmed, and is not a result of the uncertainties outlined above, it would be tempting to associate the modest LSNR to the small bulge of M94 (Möllenhoff et al. 1995). In this regard, several studies of the spatial distribution of novae in the nearby spiral M31 have suggested that the novae are primarily associated with the galaxy’s bulge (e.g. Ciardullo et al. 1987; Shafter & Irby 2001; Darnley et al. 2006). These results were somewhat surprising given the predictions of the Yungelson et al. (1997) population synthesis models, but may have an alternative explanation. In particular, Ciardullo et al. (1987) were first to put forward the idea that the high nova rate in M31’s bulge might be explained by a population of novae spawned in that galaxy’s globular cluster system and subsequently ejected into the bulge by three-body interactions within the clusters, or by tidal disruption of the clusters, or both. While extremely speculative, this process might also explain the high nova rate found by Shara & Zurek (2002) for M87, a galaxy with an unusually high specific frequency of globular clusters. Further study of the possible correlation of a galaxy’s LSNR and its specific frequency of globular clusters should be undertaken to explore this intriguing possibility more thoroughly.

## 5. Conclusions

A three-year H $\alpha$  survey of M94 spanning seven independent epochs yields the detection of four nova candidates. One of the nova candidates appeared to fade quite slowly, and may be another type of transient source. Assuming all four nova candidates are in fact novae, we estimate the annual nova rate of M94 to be  $5.0_{-1.4}^{+1.8} \text{ yr}^{-1}$ , by using a Monte Carlo simulation. The corresponding LSNR of M94 is  $1.4 \pm 0.5$  novae per year per  $10^{10} L_{\odot,K}$ , when the  $K$  magnitude is obtained from the  $(B - K)$  color and the total  $B$  magnitude. When the  $K$  magnitude is derived from 2MASS the LSNR value is little changed at  $1.5 \pm 0.4$  novae per year per  $10^{10} L_{\odot,K}$ .

Uncertainties in the measurement of nova rates in spiral galaxies arise mainly due to our difficulty in accurately determining the effects of extinction internal to the galaxy. The LSNR determined for M94 is slightly below the typical value of  $(2 - 3) \times 10^{-10} L_{\odot,K}^{-1} \text{ yr}^{-1}$  for galaxies with measured nova rates but is consistent within the uncertainty of our measurements. Though the values for the Magellanic Clouds are about 2–3 times greater than the mean LSNR value, generally there does not seem to be a strong dependence of the LSNR with different Hubble types. The higher LSNRs of the Magellanic Clouds provide support for the population synthesis models which predict that low-mass, late-type galaxies are more likely to have a higher production of novae than high-mass, early-type galaxies.

Future observations should focus on achieving more frequent temporal sampling that will improve the determination of nova rates. Dedicated surveys such as those carried out by PanStarrs and the LSST will be very helpful in this regard. Such surveys will not only help to obtain a larger sample of light curves to be used in the Monte Carlo simulations but also reduce uncertainties in the measurements of the effective survey time. It will also allow us to better assess the possible effect of stellar population on nova light curve properties.

We thank an anonymous referee for helpful suggestions to improve the paper. A.W.S. gratefully acknowledges support through NFS grant AST 06-07682.

## REFERENCES

- Ciardullo, R., Ford, H. C., Neill, J. D., Jacoby, G. H., & Shafter, A. W. 1987, ApJ, 318, 520
- Alard, C. & Lupton, R. H. 1998, ApJ, 503, 325
- Ciardullo, R., Ford, H. C., Williams, R. E., Tamblyn, P., & Jacoby, G. H. 1990a, AJ, 99, 1079
- Ciardullo, R., Shafter, A. W., Ford, H. C., Neill, J. D., Shara, M. M., & Tomaney, A. B. 1990b, ApJ, 356, 472
- Coelho, E. A., Shafter, A. W., & Misselt, K. A. 2008, ApJ, 686, 1261

- Darnley, M. J. et al. 2006, MNRAS, 369, 257
- Della Valle, M., Rosino, L., Bianchini, A., & Livio, M. 1994, A&A, 287, 403
- de Vaucouleurs, G., de Vaucouleurs, A., Corwin, H. G., Jr., Buta, R. J., Paturel, G., & Fouque, P. 1991, Third Reference Catalogue of Bright Galaxies (New York: Springer)
- Ferrarese, L., Côté, P., & Jordán, A. 2003, ApJ, 599, 1302
- Gavazzi, G. & Scodreggio, M. 1996 A&A, 312, L29
- Herrmann, K. A., Ciardullo, R., Feldmeier, J. J., & Vinciguerra, M. 2008, ApJ, 638, 630
- Jarrett, T. H., Chester, T., Cutri, R., Schneider, S. E., & Huchra, J. P. 2003, AJ, 125, 525
- Johnson, H. L. 1966, ApJ, 143, 187
- Kolb, U. 1995, in Cataclysmic Variables, ed. A. Bianchini & M. Della Valle (ASSL Vol. 205; Dordrecht: Kluwer), 511
- Livio, M. 1992, ApJ, 393, 516
- Möllenhoff, C., Matthias, M., & Gerhard, O. E. 1995, A&A, 301, 359
- Moses, R. N., & Shafter, A. W. 1993, BAAS, 25, 1248
- Neill, J. D., & Shara, M. M. 2004, AJ, 127, 816
- Oke, J. B. 1974, ApJS, 27, 21
- Prialnik, D., Livio, M., Shaviv, G., & Kovetz, A. 1982, ApJ, 257, 312
- Ritter, H., Politano, M., Livio, M., & Webbink, R. F. 1991, ApJ, 376, 177
- Schegel, D. J., Finkbeiner, D. P., & Davis, M. 1998, ApJ, 500, 525
- Shafter, A. W., Ciardullo, R., & Pritchett, C. J. 2000, ApJ, 530, 193
- Shafter, A. W., & Irby, B. K. 2001, ApJ, 563, 749
- Shara, M. M., Prialnik, D., & Shaviv, G. 1980, ApJ, 239, 586
- Shara, M. M., & Zurek, D. R. 2002, in AIP Conf. Proc. 637, Classical Nova Explosions, ed. M. Hernanz & J. Jose (Melville: AIP), 457
- Tutukov, A. V., & Yungelson, L. R. 1995, in Cataclysmic Variables, ed. A. Bianchini & M. Della Valle (ASSL Vol. 205; Dordrecht: Kluwer), 495

Waller, W. H., Fanelli, M. N., Keel, W. C., Bohlin, R., Collins, N. R., Madore, B. F., Marcum, P. M., Neff, S. G., O'Connell, R. W., Offenber, J. D., Roberts, M. S., Smith, A. M., & Stecher, T. P. 2001, *AJ*, 121, 1395

Warner, B. 1995, *Cataclysmic Variable Stars* (Cambridge: Cambridge Univ. Press)

Williams, G. G., Olszewski, E., Lesser, M. P., & Burge, J. H. 2004, *Proc. SPIE*, 5492, 787

Williams, S. J., & Shafter, A. W. 2004, *ApJ*, 612, 867

Yungelson, L., Livio, M., & Tutukov, A. 1997, *ApJ*, 481, 127

Zwicky, F. 1942, *ApJ*, 96, 28

Table 1. Summary of Observations

UT Date	Julian Date (2,450,000+)	Number of Exposures	Total Integration Time (hr)
2005 May 01.....	3491.5	10	2.5
2005 May 02.....	3492.5	2	0.5
2005 May 30.....	3520.5	5	1.25
2005 May 31.....	3521.5	3	0.75
2006 Apr 19.....	3844.5	11	2.75
2006 May 24.....	3879.5	11	2.0
2006 Jun 17.....	3903.5	10	1.67
2007 Mar 10.....	4169.5	18	3.0
2007 Jun 08.....	4259.5	18	3.0

Table 2. Magnitudes and Positions of M94 Nova Candidates

Nova	Julian Date (2,450,000+)	$\alpha$ (J2000.0)	$\delta$ (J2000.0)	$\Delta r$ (arcmin)	$m_{H\alpha}$ (mag)
M94N 2005-05a	3520.5	12 51 04.3	41 06 41	2.18	19.7
M94N 2006-04a <sup>a</sup>	3844.5	12 50 54.4	41 09 08	1.94	20.7
	3879.5	...	...	...	21.3:
	3903.5	...	...	...	21.2
M94N 2006-04b	3844.5	12 50 44.7	41 08 23	1.97	20.0
	3879.5	...	...	...	21.1:
	3903.5	...	...	...	20.9
M94N 2006-06a	3903.5	12 50 36.8	41 04 20	4.22	19.8

Note. — The units for right ascension are hours, minutes, and seconds. The units for declination are degrees, arcminutes, and arcseconds. We assume these values to be accurate to  $\sim 1''$ . The distance between the center of M94 and the nova is defined as  $\Delta r$ .

<sup>a</sup>Slowly fading transient source that is possibly a long-period variable star.

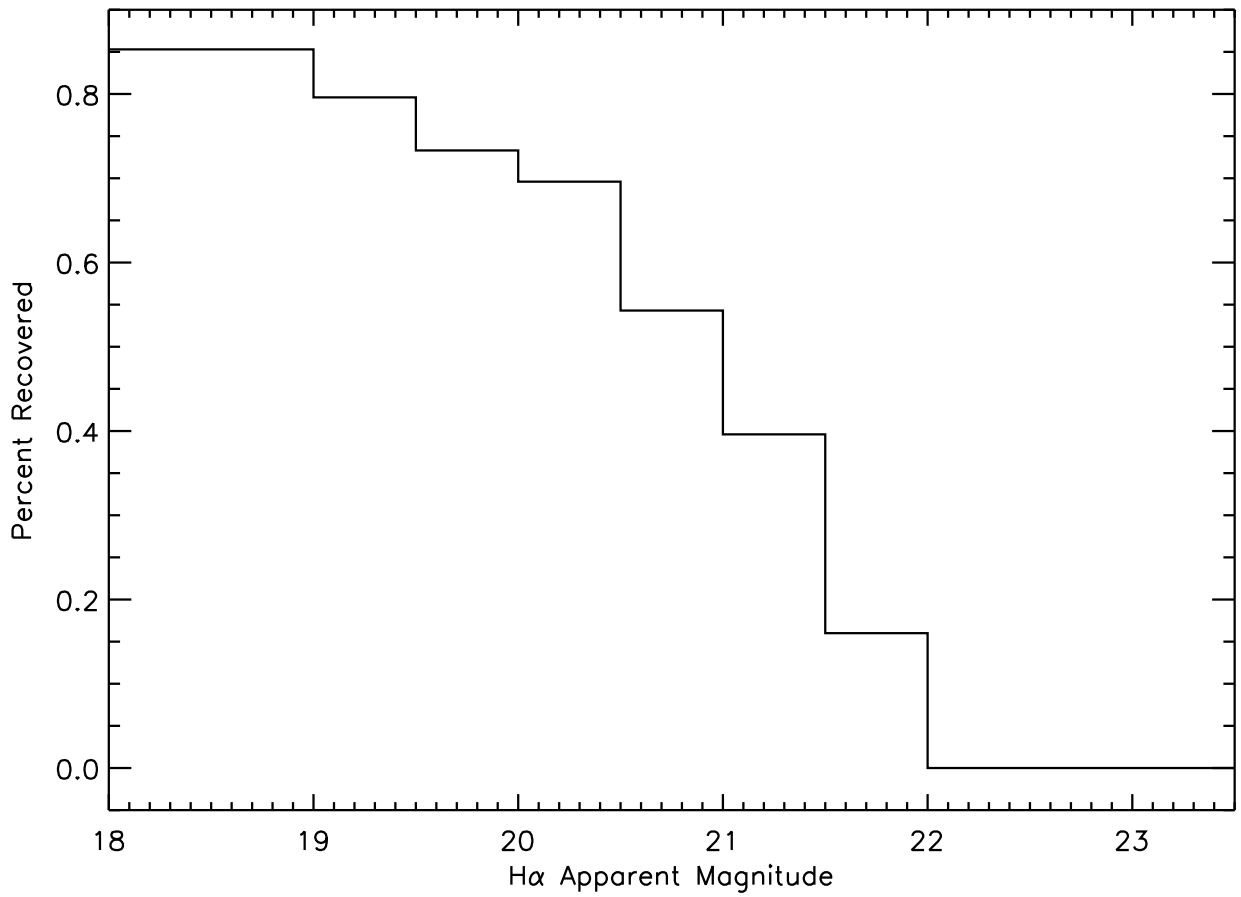


Fig. 1.— Fraction of artificial novae recovered during artificial star tests as a function of magnitude,  $C(m)$ . The limiting magnitude of  $m_{\text{H}\alpha} = 21.0$ , which is used in the mean lifetime nova rate calculation, is determined by the steep drop-off in completeness at fainter magnitudes.

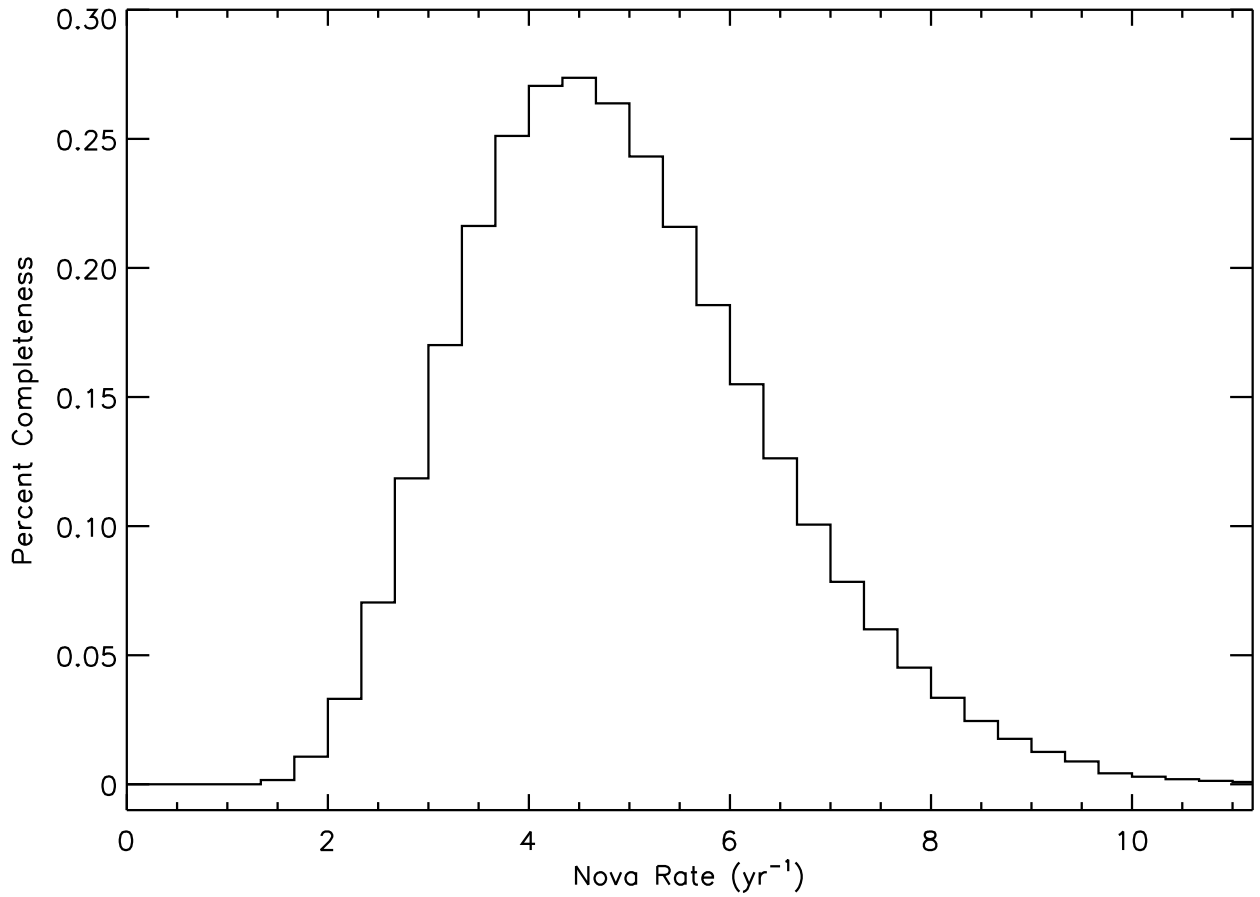


Fig. 2.— Results from the Monte Carlo simulation for the four nova candidates. The peak in the normalized probability distribution ( $R = 4.7 \text{ yr}^{-1}$ ) represents the most probable nova rate in M94 within the surveyed region of the galaxy.



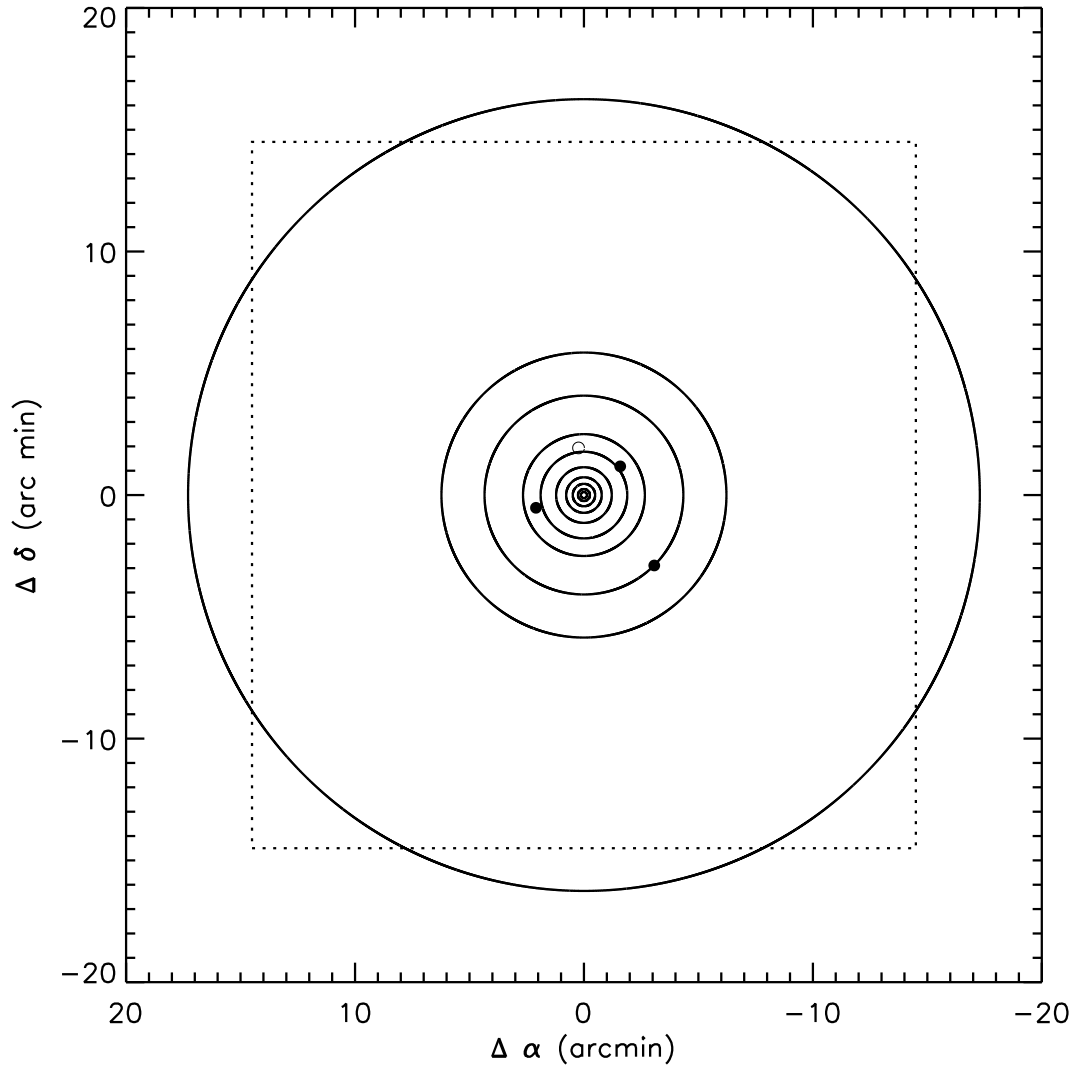


Fig. 3.— Spatial distribution of the four nova candidates found in M94. All four objects were found to be above the limiting magnitude of  $m_{H\alpha} = 21.0$ . The open circle represents a questionable source that could possibly be a long-period variable star masquerading as a nova. Also shown are the mean  $I$ -band isophotes obtained from Möllenhoff et al. (1995) and the sampled region of this survey, defined by the dashed box centered on the nucleus of the galaxy.

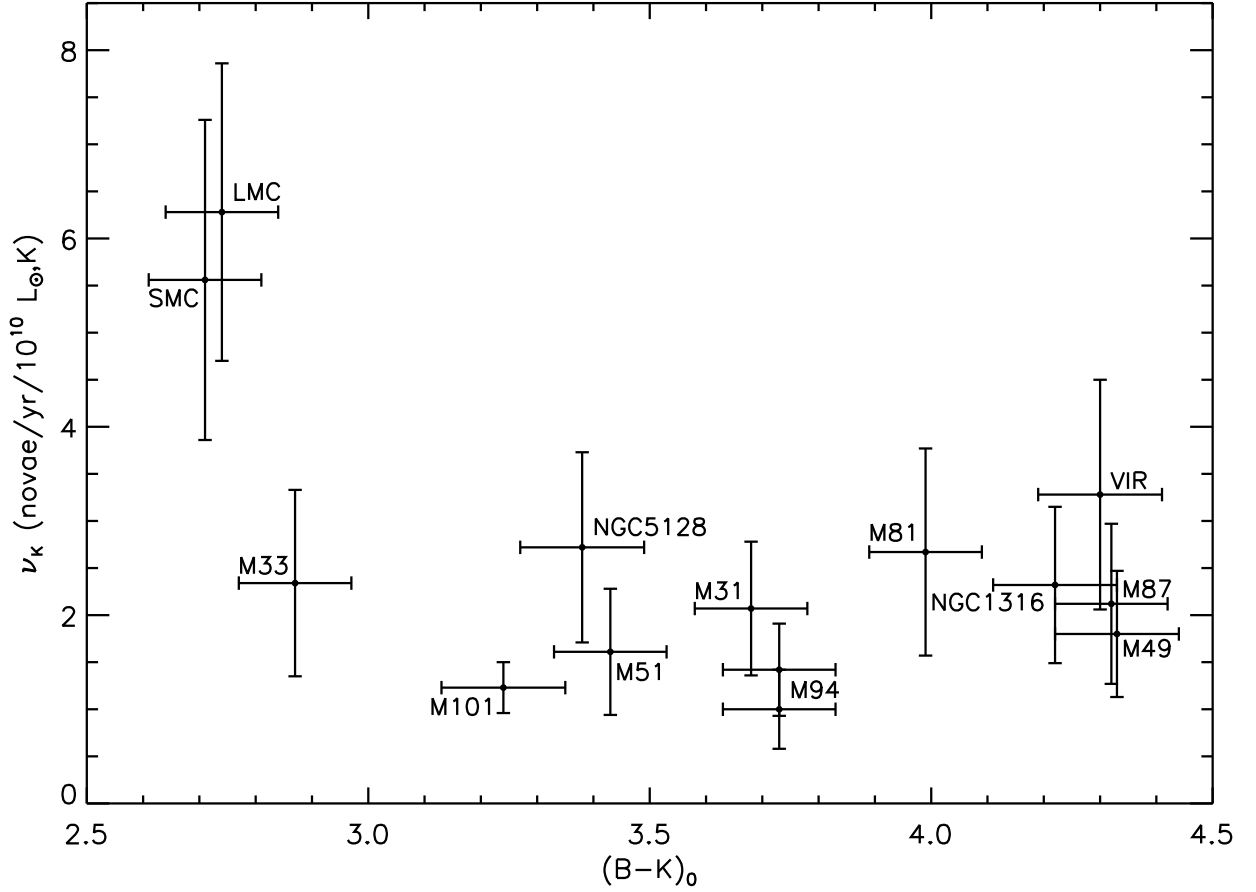


Fig. 4.— LSNRs of surveyed galaxies are plotted as a function of the  $(B - K)$  color of the galaxy. Most galaxies have LSNRs values that are close to a typical value of  $\nu_K \sim (2 \pm 1) \times 10^{-10} L_{\odot,K}^{-1} \text{ yr}^{-1}$ . We have plotted two points for M94 representing the LSNR based on the detection of either three or four novae. Note that the two low-mass, late-type irregular Magellanic Clouds have LSNRs that are  $\sim 2$ – $3$  times greater.